

A Simple and Effective Method of Evaluating Atomic Force Microscopy Tip Performance

H.-Y. Nie* and N. S. McIntyre

Surface Science Western, The University of Western Ontario,
London, Ontario N6A 5B7, Canada

Received July 21, 2000. In Final Form: October 31, 2000

The morphology of a surface imaged by dynamic force mode atomic force microscopy is obtained through an interaction between the probe tip and surface features. When the tip is contaminated and the size of the contaminant is comparable to the size of the features on the sample surface, artifacts attributable to the contaminant are observed to dominate the image. To reduce the possibility of effects from such artifacts, the tip performance should be checked by scanning a reference sample of known surface morphology. We demonstrate a simple and effective method of evaluating tip performance by the imaging of a commercially available biaxially oriented polypropylene (BOPP) film, which contains nanometer-scale-sized fibers. This sample is appropriate for use as a reference because a contaminated tip will not detect the fiberlike network structure. In addition, BOPP has a soft, highly hydrophobic surface of low surface energy, thus ensuring that the tip will not be damaged or contaminated during the evaluation process.

Introduction

In dynamic force mode atomic force microscopy (AFM), an image of the surface morphology is obtained by maintaining the cantilever in a reduced constant oscillating amplitude as the tip scans the sample surface.^{1–4} In this mode, the tip taps the sample or is in intermittent cyclical contact with the sample. One of the advantages to dynamic force mode AFM is that the lateral forces can be largely eliminated as compared to contact mode AFM, where the tip mechanically contacts the sample and the shearing force induced by the scanning of the tip on the sample surface may easily degrade the surface.³

Because dynamic force mode AFM morphology is derived from the interaction between the tip and surface features, it is clear that the size of the tip apex is a determining factor in ascertaining how closely the measured morphology matches real surface features, especially when the sizes of the tip apex and the surface feature are comparable. Simulations of the tip effect on AFM images⁵ and techniques for the deconvolution of tip-affected AFM images⁶ have been reported. However, in practice, it is clear that the tip performance should be checked by scanning a reference sample with well-known surface features.

When the tip is contaminated, the contaminant on the tip apex will most likely dominate the interaction between the sample surface and the tip and result in images displaying the convoluted effect of the surface features and the contaminant. Therefore, to ensure that the surface morphology imaged by AFM is “true”, the tip should be checked for contamination or damage. We suggest in this paper that a biaxially oriented polypropylene (BOPP)

film^{7–11} is an ideal system to evaluate the performance of the tip. This polymer film is characterized by nanometer-scale fine fiber structures,^{9,10} which as we demonstrate are especially suitable for checking the performance of tips. We show, in this work, that when using a contaminated tip, the fine fibers presented a totally different appearance, which is a reflection of the contaminant on the tip apex. We were able to “contaminate” a tip by scanning a UV/ozone-treated and subsequently water-washed BOPP surface. This contaminated tip was subsequently used to scan an untreated BOPP film, and then the tip was cleaned after the first image by pushing the tip into the polymer film, during which the amplitude–distance curve was monitored. We then imaged the same location again after the tip was cleaned to see the artifacts in the image which had been induced by the contaminant on the tip apex.

Recently, it has been noted that the change in the amplitude of oscillation of the cantilever versus the tip–sample separation can provide information about the interaction between the tip and surface, such as the attractive and repulsive forces exerted between them.^{3,12–17} We apply this measurement of the amplitude–distance curve to detect the presence of contaminant on the tip apex.

Because the polymer film is soft compared to the silicon tip (Young's modulus for polypropylene is 1–2 GPa,¹⁸ while

(1) Zhong, Q.; Inniss, D.; Kjoller, K.; Elings, V. B. *Surf. Sci.* **1993**, *290*, L688.

(2) Spatz, J. P.; Sheiko, S.; Moller, M.; Winkler, R. G.; Reineker, P.; Marti, P. *Nanotechnology* **1995**, *6*, 40.

(3) Tamayo, J.; Garcia, R. *Langmuir* **1996**, *12*, 4430.

(4) Burnham, N. A.; Behrend, O. P.; Oulevey, F.; Gremaud, G.; Gallo, P.-J.; Gourdon, D.; Kulik, A. J.; Pollock, H. M.; Briggs, G. A. D. *Nanotechnology* **1997**, *8*, 67.

(5) Komiyama, M.; Ohkubo, S.; Tazawa, K.; Tsujimichi, K.; Hirofumi, A.; Kubo, M.; Miyamoto, A. *Jpn. J. Appl. Phys.* **1996**, *35*, 2318.

(6) Tabet, M. F.; Urban III, F. K. *J. Vac. Sci. Technol., B* **1997**, *15*, 800.

(7) Nie, H.-Y.; Walzak, M. J.; Berno, B.; McIntyre, N. S. *Appl. Surf. Sci.* **1999**, *144–145*, 627.

(8) Nie, H.-Y.; Walzak, M. J.; McIntyre, N. S.; El-Sherik, A. M. *Appl. Surf. Sci.* **1999**, *144–145*, 633.

(9) Nie, H.-Y.; Walzak, M. J.; Berno, B.; McIntyre, N. S. *Langmuir* **1999**, *15*, 6484.

(10) Nie, H.-Y.; Walzak, M. J.; McIntyre, N. S. *Polymer* **2000**, *41*, 2213.

(11) Nie, H.-Y.; Walzak, M. J.; McIntyre, N. S. In *Surface Modification: Relevance to Adhesion*; Mittal, K. L., Ed.; VSP: Utrecht, The Netherlands, 2000; Vol. 2, p 377.

(12) Kuhl, A.; Sorensen, H.; Bohr, J. *J. Appl. Phys.* **1997**, *81*, 6562.

(13) Anczykowski, B.; Cleveland, J. P.; Kruger, D.; Elings, V.; Fuchs, H. *Appl. Phys. A* **1998**, *66*, S885.

(14) Garcia, R.; Paulo, A. S. *Phys. Rev. B* **1999**, *60*, 4961.

(15) Ohnesorge, F. M. *Surf. Interface Anal.* **1999**, *27*, 379.

(16) Stapff, I.; Weidmann, G.; Schellenberg, C.; Regenbrecht, M.; Akari, S.; Antonietti, M. *Surf. Interface Anal.* **1999**, *27*, 392.

(17) Durig, U. *Surf. Interface Anal.* **1999**, *27*, 467.

for silicon it is 132–190 GPa^{19–21}), the polymer will not damage the tip when the tip is pushed into the polymer. Another important property of BOPP is that the polymer film is highly hydrophobic and has a very low surface energy of ~ 30 mJ/m².^{22–24} These properties prevent contaminants from accumulating on the surface, and hence scanning the tip across the surface will likely not contaminate the tip. This belief is supported by our own extensive experience of imaging BOPP films, where we have not encountered tip contamination or damage. The experimental results we present in this paper suggest that the BOPP film is a simple and effective reference sample for checking tips to avoid any possible artifacts caused by contaminants on the tip apex or the mechanical damage of the tip.

Methods and Materials

A silicon cantilever with nominal geometric dimensions of 130 μm length, 29 μm width, and 3.7 μm thickness was used in this study. The nominal spring constant was ~ 30 N/m. The tip was approximately 10 μm high with a nominal tip apex radius of 20 nm. The dynamic force mode atomic force microscope (Topo-Metrix's Explorer) was employed for the experiments. In this study, the cantilever was oscillated at its resonant frequency (~ 280 kHz) with a high oscillation amplitude of ~ 40 nm in free space (the tip is far enough away from the sample where there is no interaction between the tip and the sample) as estimated following the method described in the literature.¹² The amplitude of the oscillation decreases as the tip is brought sufficiently close to the surface so that the tip "feels" attractive and repulsive forces. The cantilever was set at a specific distance from the sample surface where the oscillation amplitude was reduced to half (50%) the observed amplitude in free space. The AFM image obtained at this set point of the amplitude, with a scan rate of 10 $\mu\text{m/s}$, consisted of 500 lines with 500 pixel points per line. Amplitude–distance curves are obtained by measuring the amplitude of the oscillation of the cantilever as the tip is brought close to and then retracted from the surface at a speed of 100 nm/s.

A commercially available, thermally extruded, biaxially oriented isotactic polypropylene film (0.3 mm thick) was used in this study. The BOPP film was produced from a homopolymer resin (molecular weight $M_w = 1.9 \times 10^5$, polydispersity 6.0). The base resin contains 500–1000 ppm each of an inorganic acid scavenger and a high-molecular-weight phenolic antioxidant. The BOPP film was produced on a tenter frame film line and quenched at 45 °C prior to orientation. The machine direction draw ratio was 5.2:1, and the transverse direction draw ratio was 9:1. The film was converted in a direction identical to the machine direction.

To demonstrate the effect of imaging using a contaminated tip, we need to contaminate and then clean the tip and scan the same location of the polymer surface. A UV/ozone-treated and subsequently water-washed BOPP film^{25,26} was a convenient contaminant source for the tip. The BOPP film was treated in ozone in the presence of UV light for 45 min and then washed with water for 30 min. On the surface of the sample, a tiny amount of oxidized material can be easily transferred onto the tip apex in the course of scanning. The detection of the contaminant on

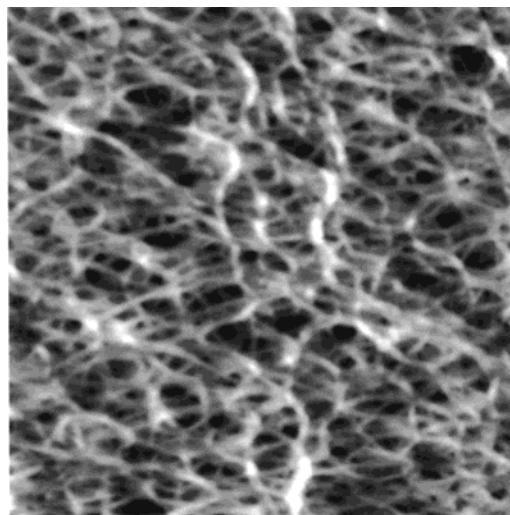


Figure 1. AFM image (scan area 2 $\mu\text{m} \times 2 \mu\text{m}$) of a BOPP film imaged by dynamic force mode AFM using the original uncontaminated tip. The gray scale range is from 0 to 20 nm.

the tip was accomplished by observing the sudden change in the image quality. The contaminated tip can be cleaned by pushing the tip several times into an untreated BOPP film.

Results and Discussion

The typical morphology of the original BOPP film is shown in Figure 1, in which nanometer-scale fine fiber structure is clearly seen. The fibrous structure is formed by the bidirectional stretching process for making the polymer film.^{9,10} Our experience in imaging the BOPP film indicates that these nanometer-scale fiberlike features are not seen when the tip is contaminated. It was this characteristic that led us to use BOPP as a reference. To demonstrate how an AFM image of the BOPP surface changes because of the contamination of the tip apex, we needed to find a quick and reproducible "contaminant source". For our purposes, this contaminant needs to be removed easily so that we can observe the tip effect on images. When a tip was used to scan a water-washed UV/ozone-treated BOPP surface, it was easily and reproducibly contaminated due to the nature of the hydrophilic materials on this surface. We used this treated surface to "contaminate" the tip to demonstrate the effect on the fiberlike features in the image of the BOPP film.

The image of the BOPP film, collected with a contaminated tip, is shown in Figure 2a. It is evident that the image is dominated by similar moundlike structure and that the fiberlike structure is not seen. Then the tip was cleaned by pushing it into the BOPP surface several times while measuring the amplitude–distance curves. This was found to be an effective way to clean the contaminated tip. The removal of the contaminant from the tip apex was indicated by the recorded amplitude–distance curves, which will be discussed later.

After cleaning, the same tip was used to obtain an image at the same location. The surface morphology is shown in Figure 2b, in which the fiberlike structure is clearly imaged. The two images obtained at the same location, by the same tip, before and after cleaning are very different in appearance. It is clear that in Figure 2a the tip effect dominates the image so that the contaminated tip itself is imaged as "artifacts" in the AFM image, not the surface features. When using a contaminated tip, detailed surface features cannot be imaged correctly. However, one can still see that the location for the two images in Figure 2 is the same one by identifying some of the larger surface features indicated by an arrow.

(18) Brostow, W.; Kubat, J.; Kubat, M. M. In *Physical Properties of Polymers Handbook*; Mark, J. E., Ed.; American Institute of Physics: New York, 1996; Chapter 23, p 331.

(19) Zhang, L. M.; Uttamchandani, D.; Culshaw, B. *Sens. Actuators, A* **1991**, 29, 79.

(20) Petersen, K. E. *Proc. IEEE* **1982**, 70, 420.

(21) Wortman, J. J.; Evans, R. A. *J. Appl. Phys.* **1965**, 36, 153.

(22) van Oss, C. J.; Chaudhury, M. K.; Good, R. J. *Sep. Sci. Technol.* **1989**, 24, 15.

(23) Wu, S. *Polymer Interface and Adhesion*; Marcel Dekker: New York, 1982; Chapter 5.

(24) Schonhorn, H.; Sharpe, L. H. *J. Polym. Sci., B* **1965**, 3, 235.

(25) Walzak, M. J.; Flynn, S.; Foerch, R.; Hill, J. M.; Karbasheski, E.; Lin, A.; Strobel, M. *J. Adhes. Sci. Technol.* **1995**, 9, 1229.

(26) Hill, J. M.; Karbasheski, E.; Lin, A.; Strobel, M.; Walzak, M. *J. J. Adhes. Sci. Technol.* **1995**, 9, 1575.

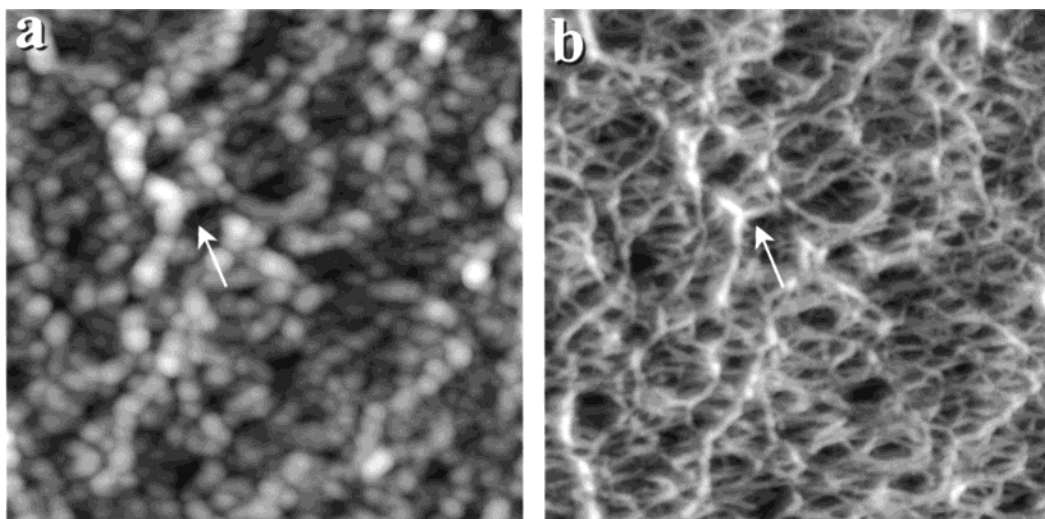


Figure 2. AFM images (scan area $2\ \mu\text{m} \times 2\ \mu\text{m}$) of a BOPP film at the same location before (a) and after (b) the tip was cleaned. The arrow indicates one of the surface features which are easily identified in both images. The gray scale range is from 0 to 18 and 22 nm for (a) and (b), respectively.

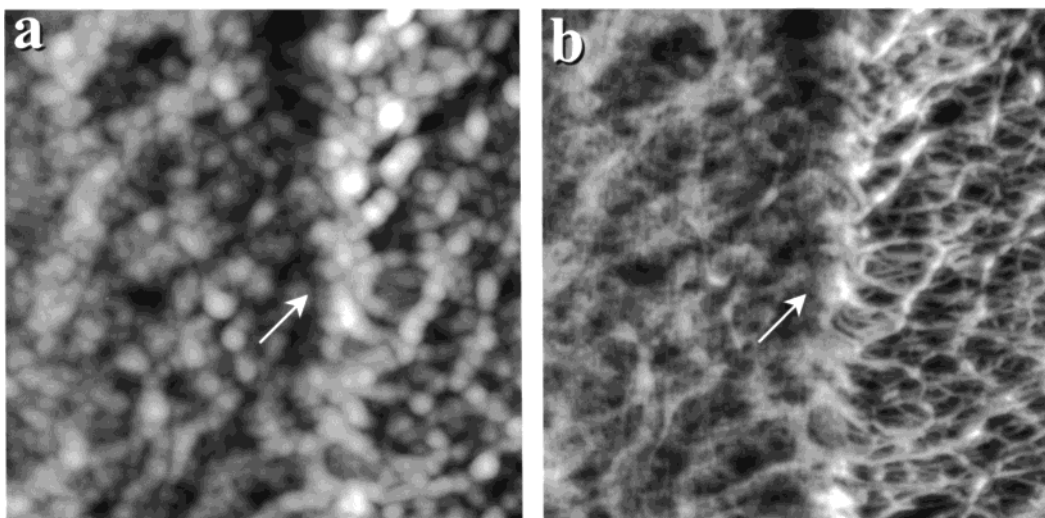


Figure 3. AFM images (scan area $2\ \mu\text{m} \times 2\ \mu\text{m}$) of a BOPP film at the same location before (a) and after (b) the tip was cleaned. The left-hand side in the image is a scratched area, where the fibers are aligned to the vertical direction. The arrow indicates the edge of the scratch which is easily identified in both images. The gray scale range is from 0 to 16 and 19 nm for (a) and (b), respectively.

A similar experiment was done at another location where a shear force deformed scratch occurred on the surface and where the fibers had aligned parallel to the shear force direction.⁹ This location was chosen because of the different surface morphologies present (i.e., both scratched and unscratched surfaces) to determine if the contaminated tip could distinguish the difference. The images collected before and after the tip was cleaned are shown in parts a and b, respectively, of Figure 3. As clearly imaged in Figure 3b by the cleaned tip, the left-hand side of the image is the scratched area showing fibers aligned in the shear force direction (vertical direction in the image) and the right-hand side is the unscratched area showing the unaligned network structure. From the image (Figure 3a) collected with the contaminated tip it was difficult to distinguish any difference in morphology between the scratched and unscratched areas. This is because the contaminant-related artifacts dominated the AFM image. The larger surface features such as the edge of the scratched area can be identified in the two images and serve as a marker for identifying the same location for the

two images. An arrow shown in both images indicates the edge of the scratched area.

The tip effect, resulting from the convolution of the surface features and contaminant on the tip apex, is clearly revealed in the two comparative images in Figure 2 or 3, which were collected at the same location with the same tip before and after the tip was cleaned. The interactive force between two bodies with radii of R_1 and R_2 is proportional to their radii as $R_1 R_2 / (R_1 + R_2)$.²⁷ In this case, R_1 and R_2 are the effective sizes of the tip and the surface features under the tip. The one with smaller size will act as the probing tip to image the other. Thus, contaminants with different volumes and shapes will result in different "signatures" for the image of the BOPP film.

A closer look of the images reveals more clearly the mechanism for the observed artifacts in the AFM images. Parts a and d of Figure 4 show magnified AFM images from Figure 3a obtained by the contaminated tip on the unscratched fibrous area and scratched area, respectively.

(27) Israelachvili, J. N. *Intermolecular and Surface Forces*, 2nd ed; Academic Press: London, 1991.

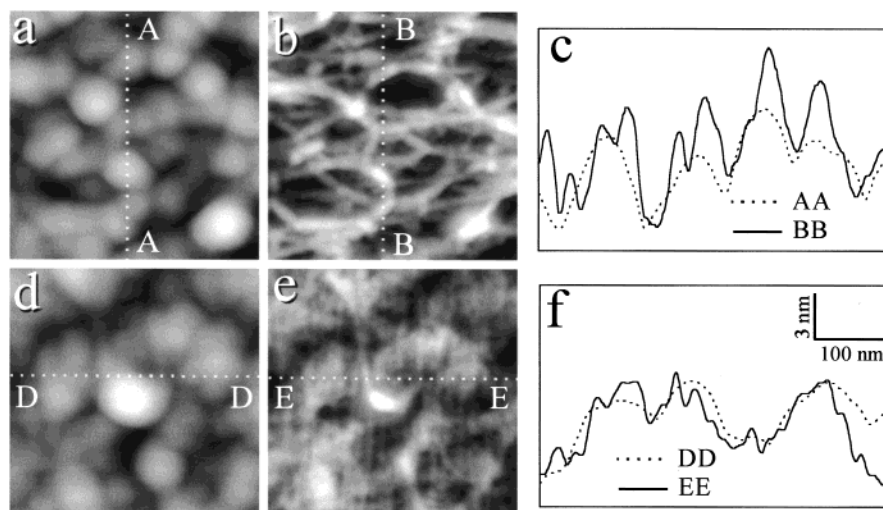


Figure 4. AFM images obtained by a contaminated tip on the fibrous structure (a) and scratched area (d). After the tip was cleaned, the images obtained at the same locations for (a) and (d) are shown in (b) and (e), respectively. The scan area for the images, which are magnified from Figure 3, is $500 \text{ nm} \times 500 \text{ nm}$. Cross-sectional profiles indicated by dashed lines AA and BB in (a) and (b) are shown in (c), while those indicated by dashed lines DD and EE in (d) and (e) are shown in (f). The inset in (f) shows the distance (horizontal) and height (vertical) scales for both (c) and (f). The gray scale range for all images is from 0 to 12 nm.

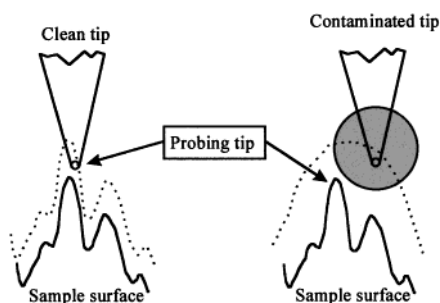


Figure 5. The different imaging results for a clean tip and a contaminated tip are schematically depicted. The radii of the tip apex and contaminant are shown by small and large circles, respectively. The relatively smaller one of the tip and the surface feature acts as the probing tip to image the other.

Images magnified from Figure 3b obtained after the tip was cleaned for the same unscratched fibrous area and the scratched area are shown in parts b and e, respectively, of Figure 4. Although the surface morphology on the unscratched bidirectional fibrous structure (Figure 4b), it is clear that similar moundlike artifacts are seen in the images collected by the contaminated tip on the two areas with different surface structures (Figure 4a,d). It is also interesting to note that the artifacts are located at higher protrusions of the surface morphology and surface features that are below those protrusions are not imaged. Therefore, the artifacts observed in the AFM images can be explained by this: the local protrusions on the surface act as probing tips to image the contaminant on the tip apex. Shown in Figure 4c,f are the cross-sectional profiles obtained by the contaminated tip (dashed line) and cleaned tip (solid line) at the same locations marked by dashed lines on images for the unscratched fibrous surface (Figure 4a,b) and scratched surface (Figure 4d,e), respectively. It is clear from Figure 4c,f that the cleaned tip images the surface features (solid line) while the contaminant itself (dashed line) on the contaminated tip is imaged by the protruding surface features.

We show schematically in Figure 5 the contaminant on the tip to explain the appearance of the observed moundlike artifacts observed in AFM images collected by the contaminated tip. On the left-hand side shows a clean tip

and the sample surface features. The apex of the clean tip has a small radius indicated by a circle. Assuming that the radius of the clean tip apex is smaller than that of the surface features, then the surface features are imaged as indicated by the dashed line. The contaminated tip is shown on the right-hand side. For simplicity of depicting the concept for the convolution effect of the tip and the surface feature, a round droplet is used to model the contaminant whose radius is indicated by the larger circle. Because the contaminant is larger than the surface features, the protrusion of the surface features acts as a probing tip to image the contaminant as indicated by the dashed line. In our case, because the height of local protrusions of the BOPP surface is quite small ($\sim 5 \text{ nm}$), only the "apex" of the contaminant is imaged. For imaging more deeply the shape of the contaminated tip, a much higher surface feature is needed. For example, a pinlike structure with a height of 300 nm presented on a deposited copper film imaged the pyramid-shaped AFM tip $\sim 1 \mu\text{m}$ deep from the apex.²⁸

For the cleaning process involved in obtaining images shown in Figures 2b and 3b, it is useful to determine the mechanism of cleaning when the tip was pushed into the BOPP film. By measuring the amplitude–distance curves, the process of contaminant removal from the tip can be monitored. Shown in Figure 6 are the amplitude–distance curves measured after the image shown in Figure 2a was obtained. For clarity we only show the first and last ones of the four amplitude–distance curves obtained. The amplitude is normalized to the observed amplitude in free space. The origin of the distance is taken at a separation between the tip and the sample surface where the amplitude is reduced nominally 50%.

The first amplitude–distance curve shows that when the tip approaches the surface, the amplitude (open circles) decreases until the tip is brought so close to the surface that the amplitude is damped to zero, indicating a mechanical contact between the tip and surface. After this formation of contact, the tip was pushed $\sim 30 \text{ nm}$ further into the polymer surface. Then the tip was retracted from the surface, and the amplitude (filled circles) shows a small hysteresis of recovery from where it became zero. This hysteresis is likely due to the adhesion

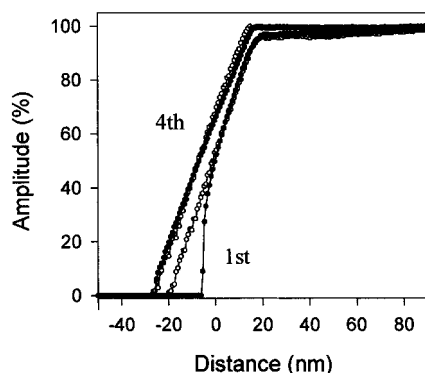


Figure 6. Four amplitude–distance curves were measured after the BOPP film surface shown in Figure 2a was imaged. For clarity only the first and fourth curves are shown, between which are the second and third curves. After the amplitude–distance measurement, the tip was used to obtain the image shown in Figure 2b. The amplitude versus the tip–sample separation when the tip is brought to and retracted from the sample surface is represented by open and filled circles, respectively. The speed of the tip movement was 100 nm/s.

force between the contaminant and the surface. When this was repeated three more cycles, the hysteresis decreased and finally vanished. In fact, this last amplitude–distance curve resembled the one obtained using the original uncontaminated tip.

We discuss a possible mechanism for the removal of the contaminant from the tip apex. When the contaminated tip is in contact with the BOPP surface during the amplitude–distance measurement, as the amplitude approaches zero, the contaminant is squeezed between the tip and the sample surface. Because the surface energy of the BOPP film is much lower than that of the silicon tip, on which exists a silicon oxide layer, we speculate that the contaminant is displaced on the wall of the tip, rather than on the BOPP sample surface.

From changes in images shown in Figures 2 and 3 and amplitude–distance curves in Figure 6, it is clear that

the contaminant transferred onto the tip by scanning the UV/ozone-treated and subsequently water-washed BOPP film has a very tiny volume. For “naturally” contaminated tips in air, images of much worse quality were obtained compared to those shown in Figures 2a and 3a, and a severe hysteresis in the amplitude–distance curves was observed. When the contaminant on the tip apex had a strong interaction with the surface, step- or peaklike features were noted in the amplitude–distance curves. The observed images were noisy because of unstable changes of amplitude during scanning due to the strong interaction between the contaminant on the tip and the sample surface.

In the present series of experiments, contamination was modeled by polymer remnants from a UV/ozone-treated and subsequently water-washed BOPP surface, which can be removed by pushing the tip into an untreated BOPP film so that an identical location to study the tip effect is available. In practice, however, contaminated tips are usually cleaned by exposure to a UV/ozone environment, which is effective in decomposing and removing organic contaminants such as hydrocarbons.

Conclusions

We demonstrated that a BOPP film characterized by the nanometer-scale fiberlike structure is a simple and effective reference sample for checking the performance of tips used in dynamic force mode AFM. The very fine fiberlike structure of the BOPP film surface is a good criterion for the tip performance. The important properties of the polymer film as a reference sample are that (1) the material is soft so that the silicon tip will not be damaged and (2) the surface is highly hydrophobic with very low surface energy so that the surface is clean enough to prevent the tip from being contaminated during scanning.

Acknowledgment. We thank M. J. Walzak for useful discussion on UV/ozone treatment of polymer surfaces.

LA001035F